ISSN 2070-0482, Mathematical Models and Computer Simulations, 2023, Vol. 15, Suppl. 1, pp. S64–S77. © Pleiades Publishing, Ltd., 2023.
Russian Text © The Author(s), 2023, published in Matematicheskoe Modelirovanie, 2023, Vol. 35, No. 7, pp. 97–117.

Numerical Simulation of Dynamic Processes in the Medium of Fine-Grained Solid Particles

M. Y. Nemtsev[a,*]

[a] *Federal Scientific Center Scientific Research Institute of System Analysis, Russian Academy of Sciences, Moscow, Russia*

**e-mail: nemtsev@niisi.ras.ru*

Received May 11, 2023; revised June 5, 2023; accepted June 19, 2023

Abstract—A mathematical model and numerical method for solving problems of the flow of two-phase mixtures of gas and fine solid particles are considered. The particles are assumed to be absolutely rigid, incompressible, and nondeformable. As the initial model, the continuum model of R.I. Nigmatulin is considered. The model has two drawbacks: it is not strictly hyperbolic (i.e., it degenerates into an elliptical one under certain flow regimes) and has a nonconservative form, which makes it difficult to solve numerically. This paper proposes a method for regularizing Nigmatulin's model at a discrete level, which makes it possible to eliminate these shortcomings and develop a numerical model that is well-conditioned for evolutionary problems of the flow of gas-dispersed mixtures with nondeformable solid particles. The regularization method is based on splitting the original system into two subsystems, each of which is strictly hyperbolic and has a conservative form. Difference schemes of the Godunov type are developed for the numerical solution of these subsystems. Testing of the proposed model and implemented methods includes checking the preservation of a homogeneous solution and the formation of shock waves and rarefaction waves in a gas, as well as compaction and decompaction waves in the particle phase. The results of the numerical simulation of the interaction of a shock wave in a gas with a near-wall layer of particles are also presented.

Keywords: two-phase dispersed media, continuum model of an ensemble of solid particles, regularization of Nigmatulin's model, Godunov's numerical method

DOI: 10.1134/S2070048223070128

1. INTRODUCTION

In various applied and fundamental problems, there are flows of two-phase mixtures consisting of gas and solid small particles, which in the considered modes are practically absolutely rigid, incompressible, and nondeformable. Examples include powder technological processes in the chemical and food industries [1], environmental problems related to environmental pollution [2], the development of porous energy materials [3], ensuring safety, and preventing dust explosions [4]. When developing mathematical models of such two-phase mixtures, it is necessary to take into account the features of the flow: the interaction of the gas and dispersed phases both due to viscous forces and the pressure gradient in the gas, and the formation of compaction and decompaction waves in the dispersed phase, as well as vacuum zones (areas of pure gas without particles) and a number of other features. In this case, it is necessary for the mathematical model to describe all possible flow regimes, from the regime of close-packed particles, when they are in contact with each other, to the regime of rarefied particles with a very small volume fraction.

One of the first models was the Marble model [5]. It describes only the class of rarefied flows when the volume fraction of particles can be neglected. This model actually can be reduced to gas dynamics equations with a variable (depending on the mass concentration of the particles) adiabatic exponent in the equation of state.

Continuum models that take into account the volume fraction of particles and, in principle, are suitable for a wide range of flows are proposed in [6–8]. These models are based on the fundamental laws of conservation of mass, momentum, and energy; and they take into account, together with the viscous interaction of phases, the Archimedean force due to the pressure gradient in the gas. The mass conservation equation in such a model has the form of the law of conservation of the number of particles or, equivalently, the volume fraction of particles.

Although these models are widely used for practical problems, they have two significant drawbacks: they are not strictly hyperbolic and have a nonconservative form. In this case, the eigenvalues can be complex. This leads to ill-conditioned mathematical problem, instability of the numerical solution, and the introduction of additional artificial stabilization algorithms, which, as a rule, do not always solve the problem.

One of the ways to eliminate this drawback (hyperbolicity degeneration) is to use the Bayer–Nunziato (BN) equations model, in which both phases, gas and particles, are considered in the continuum approximation as two compressible continua with their own equations of state [9]. Each of these continua is described by its own system of Euler equations: a set of laws of conservation of mass, momentum, and energy. The resulting system of equations is closed by an equation for the volume fraction, which has the form of a transport equation with a certain interfacial velocity.

The eigenvalues of the BN system of equations are real and, therefore, it is hyperbolic. The disadvantage of this approach is that the dispersed phase has to be considered not as an ensemble of absolutely rigid nondeformable particles, but as some fictitious compressible medium with its own equation of state. As a rule, this equation of state is not a real equation that describes the properties of the particle material, but is selected artificially [10]. In addition, the nonconservative transport equation for the volume fraction does not guarantee the conservation of the number of particles, which is important for describing dispersed mixtures.

It should be noted that the BN model was initially proposed to describe the physicochemical processes of a densely packed granular medium at high pressures, especially when calculating the transition from deflagration to detonation in condensed explosives. For such processes, its use is justified, since the particles are in close contact with each other and can be modeled not as a dispersed medium but as some kind of porous material. In particular, the process of particle dispersion and their transition to a rarefied state with a low volume fraction is not described by the BN model. The BN model in the limiting case of a small vanishing volume fraction does not transform into the Marble model.

The second feature of the system of BN equations is the behavior at a slightly varying density of the dispersed phase. In this case, the law of conservation of mass leads to a balance equation for the number of particles, which has a nondivergent form and thus contradicts the law of conservation of the number of particles. In Nigmatullin's model, the law of conservation of the number of particles has a divergent form.

Thus, from the point of view of physics, Nigmatulin's model more adequately describes broad-ranging dynamic processes in a two-phase mixture of gas and small solid particles than the BN model. At the same time, the latter is correct in a mathematical sense for evolutionary problems. The aim of this study is to correct this shortcoming of Nigmatulin's model. To do this, we propose regularization of the model at a discrete level, which consists of splitting the original system into two subsystems, each of which is strictly hyperbolic and has a conservative form. As a result, we have a numerical model that inherits all the positive properties of Nigmatulin's physical model and corrects the shortcomings of the mathematical model.

The structure of the article is as follows. Section 2 presents the initial system of governing equations for a two-phase mixture of gas and solid particles, analyzes its thermodynamic consistency and evolutionary nature, and considers splitting it into two hyperbolic subsystems of a conservative type. Section 3 discusses numerical methods of the Godunov type for solving the constructed subsystems. In Section 4, the proposed numerical model is verified and tested on a number of one-dimensional problems related to the formation of wave structures of the compaction and decompaction of particles during shock-wave interactions.

2. SYSTEM OF GOVERNING EQUATIONS

A mathematical model is considered that describes the dynamics of a mixture of gas and solid particles in the continuum approximation [3, 7]. We will denote the parameters of the gas phase by index 1, and the parameters of the particle phase (also condensed phase, k-phase, dispersed phase) by index 2. The governing equations of the model are as follows:

$$\frac{\partial \alpha_1 \rho_1}{\partial t} + \nabla(\alpha_1 \rho_1 \mathbf{u}_1) = 0,$$

$$\frac{\partial \alpha_2}{\partial t} + \nabla(\alpha_2 \mathbf{u}_2) = 0,$$

$$\begin{gathered}\frac{\partial \alpha_1 \rho_1 \mathbf{u}_1}{\partial t} + \nabla\left(\alpha_1 \rho_1 \mathbf{u}_1 \otimes \mathbf{u}_1 + p\right) = \alpha_2 \nabla p + \mathbf{f}_1, \\ \frac{\partial \alpha_2 \rho_2 \mathbf{u}_2}{\partial t} + \nabla\left(\alpha_2 \rho_2 \mathbf{u}_2 \otimes \mathbf{u}_2 + \alpha_2 \pi\right) = -\alpha_2 \nabla p_1 + \mathbf{f}_2, \\ \frac{\partial \alpha_1 \rho_1 E_1}{\partial t} + \nabla\left(\alpha_1 \rho_1 E_1 \mathbf{u}_1 + p \mathbf{u}_1\right) = \alpha_2 \mathbf{u}_2 \nabla p + \nabla\left[p \alpha_2 \left(\mathbf{u}_1 - \mathbf{u}_2\right)\right] + \mathbf{u}_2 \mathbf{f}_1 + q_1, \\ \frac{\partial \alpha_2 \rho_2 E_2}{\partial t} + \nabla\left(\alpha_2 \rho_2 E_2 \mathbf{u}_2 + \alpha_2 \pi \mathbf{u}_2\right) = -\alpha_2 \mathbf{u}_2 \nabla p + \mathbf{u}_2 \mathbf{f}_2 + q_2,\end{gathered} \tag{1}$$

where $\alpha, \rho, \mathbf{u}, E, p$, and π denote the volume fraction, density, velocity vector, total energy, pressure, and intergranular pressure; $\mathbf{f}_k$ and q_k are the relaxation values for the phase velocities and temperatures. It is assumed that $\alpha_1 + \alpha_2 = 1$, $\mathbf{f}_1 + \mathbf{f}_2 = 0$, $q_1 + q_2 = 0$, and $\rho_2 = \text{const}$. The magnitudes of force and thermal interphase interaction are expressed as $\mathbf{f}_1 = \mu(\mathbf{u}_1 - \mathbf{u}_2)$ and $q_1 = k(T_1 - T_2)$, where the coefficients μ and k are determined by empirical dependences [3], in which T_1 and T_2 are the gas and solid phase temperatures. System (1) does not take into account the dissipative processes related to the viscosity and thermal conductivity of the gas, with the exception of the force interaction at the interface. To approximate the intergranular pressure, the following approach is used [3]:

$$\pi_2(\alpha_2) = \begin{cases} B\left[\left((1-\alpha_{2*})/(1-\alpha_2)\right)^k - 1\right], & \alpha_2 \geq \alpha_{2*}, \\ 0, & \alpha_2 < \alpha_{2*}, \end{cases} \tag{2}$$

where the parameter α_2^* determines the critical volume fraction of densely packed particles.

Note that the energy equation for the k-phase can be reduced to the equation for the internal energy of the k-phase e_2 and further transformed to an equation for the temperature of the k-phase T_2. As the latter is needed only to describe the interfacial heat transfer, this equation is not considered further.

The equation for the entropy of gas s_1 can be obtained from the subsystem of gas phase equations in the standard way. It takes the following form:

$$\alpha_1 \rho_1 T_1 \left(\frac{\partial s_1}{\partial t} + u_1 \nabla s_1\right) = \left(\mathbf{u}_2 - \mathbf{u}_1\right) \mathbf{f}_1 + q_1, \tag{3}$$

where T_1 is the gas temperature. Thus, the system of equations (1) is thermodynamically consistent, but it is not strictly hyperbolic and for some values of the flow parameters the eigenvalues of the Jacobian matrix can be complex.

2.1. Model Regularization

As noted above, Nigmatulin's model is not strictly hyperbolic. Setting up the evolutionary Cauchy problem for it is, generally speaking, not correct. It is proposed to regularize it and eliminate this drawback at a discrete level by introducing a special type of splitting at each time step of integration.

At the first stage, we can consider the movement of the mixture without taking into account the interfacial interaction; and at the second, only the interfacial interaction. Thus, at the first stage, the system of equations (1) is solved without the right-hand sides and the energy equation for the k-phase, which serves to determine the temperature of the k-phase,

$$\begin{gathered}\frac{\partial \alpha_1 \rho_1}{\partial t} + \nabla\left(\alpha_1 \rho_1 \mathbf{u}_1\right) = 0, \\ \frac{\partial \alpha_2}{\partial t} + \nabla\left(\alpha_2 \mathbf{u}_2\right) = 0, \\ \frac{\partial \alpha_1 \rho_1 \mathbf{u}_1}{\partial t} + \nabla\left(\alpha_1 \rho_1 \mathbf{u}_1 \otimes \mathbf{u}_1 + p\right) = 0, \\ \frac{\partial \alpha_2 \rho_2 \mathbf{u}_2}{\partial t} + \nabla\left(\alpha_2 \rho_2 \mathbf{u}_2 \otimes \mathbf{u}_2 + \alpha_2 \pi\right) = 0,\end{gathered} \tag{4}$$

$$\frac{\partial \alpha_1 \rho_1 E_1}{\partial t} + \nabla\left(\alpha_1 \rho_1 E_1 \mathbf{u}_1 + p\mathbf{u}_1\right) = 0,$$

and the second stage takes into account the interfacial interaction

$$\begin{gathered}
\frac{\partial \alpha_1 \rho_1}{\partial t} = 0, \\
\frac{\partial \alpha_1 \rho_1 \mathbf{u}_1}{\partial t} = \alpha_2 \nabla p + \mathbf{f}_1, \\
\frac{\partial \alpha_2 \rho_2 \mathbf{u}_2}{\partial t} = -\alpha_2 \nabla p + \mathbf{f}_2, \\
\frac{\partial \alpha_1 \rho_1 E_1}{\partial t} = \alpha_2 \mathbf{u}_2 \nabla p + \nabla\left[p\alpha_2\left(\mathbf{u}_1 - \mathbf{u}_2\right)\right] + \mathbf{u}_2 \mathbf{f}_1 + q_1, \\
\frac{\partial \alpha_2}{\partial t} = 0.
\end{gathered} \tag{5}$$

In the case under consideration, the system of equations (4) is split into equations for the dynamics of the k-phase,

$$\begin{gathered}
\frac{\partial \alpha_2}{\partial t} + \nabla \alpha_2 \mathbf{u}_2 = 0, \\
\frac{\partial \alpha_2 \rho_2 \mathbf{u}_2}{\partial t} + \nabla\left(\alpha_2 \rho_2 \mathbf{u}_2 \otimes \mathbf{u}_2 + \alpha_2 \pi\right) = 0,
\end{gathered} \tag{6}$$

which determine the solution of α_2 and $\mathbf{u}_2$, and the gas phase equations

$$\begin{gathered}
\frac{\partial \alpha_1 \rho_1}{\partial t} + \nabla\left(\alpha_1 \rho_1 \mathbf{u}_1\right) = 0, \\
\frac{\partial \alpha_1 \rho_1 \mathbf{u}_1}{\partial t} + \nabla\left(\alpha_1 \rho_1 \mathbf{u}_1 \otimes \mathbf{u}_1 + p\right) = 0, \\
\frac{\partial \alpha_1 \rho_1 E_1}{\partial t} + \nabla\left(\alpha_1 \rho_1 E_1 \mathbf{u}_1 + p\mathbf{u}_1\right) = 0,
\end{gathered} \tag{7}$$

to find the remaining components of the solution of ρ_1, $\mathbf{u}_1$, and p.

Another important property of the system of equations of the gas phase (7) should be noted, which makes it possible to construct a numerical method for its solution based on the developed methods of classical gas dynamics. Indeed, it is easy to verify that by introducing the average density $\overline{\rho}_1 = \rho_1 \alpha_1$ the system of equations of the gas phase (7) transforms into the standard system of Euler equations with respect to variables $\overline{\rho}_1$, u_1, and p. The equation of state will be reduced to

$$p = (\overline{\gamma} - 1)\overline{\rho}_1 e_1, \tag{2}$$

where $\overline{\gamma} = (\gamma - \alpha_2)/\alpha_1$. Thus, (7) can be considered as a classical system of equations of gas dynamics of a calorically perfect gas, with the only difference that the exponent depends on the spatial distribution of the volume fraction of the k-phase.

System (4) is hyperbolic and has five eigenvalues:

$$\lambda_{1,2} = u_2 \pm c_2, \quad \lambda_{3,4} = u_1 \pm c_1 \ \lambda_5 = u_1, \tag{9}$$

where for the given approximation (2)

$$c_2 = \sqrt{\pi(1 + \alpha_2 k/(1 - \alpha_2)) + \alpha_2 Bk/\rho_2(1 - \alpha_2)}, \quad c_1 = \sqrt{p(\gamma - \alpha_2)/\rho_1 \alpha_1^2}.$$

3. NUMERICAL METHOD

Spatial discretization of the equations is carried out for simplicity on a grid with a constant step h. Integer subscripts are used to denote discrete values related to cells i; for parameters at the nodal points, half-integer indices $i + 1/2$. At each time integration step, the system of equations (4) is first solved with the initial data corresponding to the solution on the lower time layer. The resulting distribution is then used

as the initial data for the system of equations (5), which is solved at the same time step and results in a solution at the upper time layer. Selecting the time step size Δt is discussed in more detail below. Due to the conservativity of systems (4), (5), the semidiscrete form of the Godunov method can be represented as

$$\frac{\partial \mathbf{q}_i}{\partial t} = -\frac{1}{h}\left[\mathbf{f}^k_{i+1/2} - \mathbf{f}^k_{i-1/2}\right], \tag{3}$$

where $\mathbf{q}_i$ is the cell's average value of the conservative vector and index $k = I, II$ refers to the numerical method for systems (4), (5), respectively, which are further called stages. At the first stage, for the time approximation, we use approach of the predictor-corrector type [11], and to increase the order of approximation in space, a subgrid reconstruction of the solution is used, leading to the standard MUSCL-type scheme. At the second stage, a first-order scheme is used.

3.1. HLL Method for the First Stage

For the system of equations (4), the conservative vector $\mathbf{q} = (\overline{\rho}_1, \overline{\rho}_1 u_1, \overline{\rho}_1 E, \overline{\rho}_2, \overline{\rho}_2 u_2)^T$, the flow vector $\mathbf{f} = (\overline{\rho}_1 u_1, \overline{\rho}_1 u_1^2 + p_1, \overline{\rho}_1 H_1, \overline{\rho}_2 u_2, \overline{\rho}_2 u_2^2 + \pi)^T$ and $H_1 = E_1 + p_1/\overline{\rho}_1$, then the Riemann problem for it is formulated as follows:

$$\begin{gathered}\frac{\partial \mathbf{q}}{\partial t} + \frac{\partial \mathbf{f}}{\partial x} = 0, \quad x \in (-\infty, +\infty), \quad t \geq 0, \\ \mathbf{q}(0,x) = \begin{cases}\mathbf{q}_L, & x \leq 0, \\ \mathbf{q}_R, & x > 0.\end{cases}\end{gathered} \tag{4}$$

An approximate solution to the HLL-type Riemann problem is constructed under the following assumptions. As a result of the decay of the initial discontinuity, a disturbed region bounded by waves s_L and s_R is formed. The disturbed region is characterized by a constant conservative vector $\mathbf{q}^*$ and flow vector $\mathbf{f}^*$. They are found from the condition of satisfying the weak form of differential equations, $\int_\gamma (\mathbf{q}dx - \mathbf{f}dt) = 0$, for any closed loop γ. For this, it is sufficient to require that the Rankine–Hugoniot conditions be satisfied on the waves s_L and s_R, which leads to the relations

$$\mathbf{q}^* = \frac{s_R \mathbf{q}_R - s_L \mathbf{q}_L + \mathbf{f}_L - \mathbf{f}_R}{s_R - s_L}, \quad \mathbf{f}^* = \frac{s_R \mathbf{f}_L - s_L \mathbf{f}_R + s_L s_R (\mathbf{q}_R - \mathbf{q}_L)}{s_R - s_L}. \tag{12}$$

We estimate the bounding wave velocities s_L and s_R as follows. We use the estimate [12] for the subsystem of gas phase equations (7)

$$s_{1,L} = \min\left[0, \min(\overline{u}_1 - \overline{c}_1, u_{1,L} - c_{1,L})\right], \quad s_{1,R} = \max\left[0, \max(\overline{u}_1 + \overline{c}_1, u_{1,R} + c_{1,R})\right], \tag{5}$$

where the overline denotes the mean values, $\overline{u}_1 = 0.5(u_{1,L} + u_{1,R})$, and $\overline{c}_1 = 0.5(c_{1,L} + c_{1,R})$. For the subsystem of the condensed phase equations (6), we estimate according to [13] as follows:

$$\begin{gathered}\tilde{\alpha}_2 = \max(\alpha_{2,L}, \alpha_{2,R}), \\ \tilde{u}_2 = \begin{cases}\dfrac{u_{2,L}\sqrt{\alpha_{2,L}} + u_{2,R}\sqrt{\alpha_{2,R}}}{\sqrt{\alpha_{2,L}} + \sqrt{\alpha_{2,R}}}, & \alpha_{2,L} > 0 \text{ or } \alpha_{2,R} > 0, \\ 0, \quad \text{otherwise}, \end{cases} \\ \tilde{c}_2 = c_2(\tilde{\alpha}_2), \\ s_{2,L} = \min(\tilde{u}_2 - \tilde{c}_2, u_{2,L} - c_{2,L}, -\varepsilon), \quad s_{2,R} = \max(\tilde{u}_2 + \tilde{c}_2, u_{2,R} + c_{2,R}, \varepsilon).\end{gathered} \tag{14}$$

Finally, the velocities of the confining waves are determined as extreme values of the velocities of propagation of disturbances through the gas and dispersed phase

$$s_L = \min\left[s_{1,L}, s_{2,L}\right], \quad s_R = \max\left[s_{2,R}, s_{2,R}\right]. \tag{15}$$

Then the corresponding value of the numerical flow in the approximate Godunov method takes the form

$$\mathbf{f}^I_{i+1/2}(\mathbf{z}^-, \mathbf{z}^+) = \mathbf{f}^*(\mathbf{z}^-, \mathbf{z}^+), \tag{16}$$

where $\mathbf{z}^-$ and $\mathbf{z}^+$ are approximated values of the primitive variables [13]. The scheme used is an explicit two-step one. It is stable under the Courant condition, which in this case is written as

$$\Delta t \le (h/(\max(s_{L,i}, s_{R,i}))) \quad \text{for all } i. \tag{17}$$

3.2. Flow Form of the HLL Method for the Second Stage

The solution of the split system (4), which does not take into account the interphase interaction, serves as the initial data for the interphase interaction subsystem (5), which is solved at the time step Δt. This system has the first integrals

$$\begin{gathered}\alpha_k = \alpha_k(x),\\ \rho_k = \rho_k(x),\\ \alpha_1\rho_1\mathbf{u}_1 + \alpha_2\rho_2\mathbf{u}_2 = \mathbf{const}(x).\end{gathered} \tag{18}$$

The equation for the total energy of the gas is rewritten in the form of equations for the internal energy

$$\frac{\partial\alpha_1\rho_1 e_1}{\partial t} = p\nabla[\alpha_2(\mathbf{u}_1 - \mathbf{u}_2)] + (\mathbf{u}_2 - \mathbf{u}_1)\mathbf{f}_1 + q_1. \tag{19}$$

By introducing the mass-average velocity of the mixture and the relative velocity of the phases

$$\overline{\rho}\mathbf{u} = \overline{\rho}_1\mathbf{u}_1 + \overline{\rho}_2\mathbf{u}_2, \quad \mathbf{w} = \mathbf{u}_2 - \mathbf{u}_1, \tag{20}$$

where $\overline{\rho} = \overline{\rho}_1 + \overline{\rho}_2$ and $\overline{\rho}_k = \rho_k\alpha_k$, the equation for the relative velocity is transformed

$$\frac{\overline{\rho}_1\overline{\rho}_2}{\overline{\rho}}\frac{\partial\mathbf{w}}{\partial t} = -\alpha_2\nabla p + \mathbf{f}_2. \tag{21}$$

Taking into account $\rho_1(\partial e_1/\partial p)_{\rho_1} = 1/\Gamma$, where Γ is the Mu–Grüneisen coefficient (for an ideal gas, $\Gamma = \gamma - 1$), (19) will be rewritten in the form

$$\frac{\alpha_1}{\Gamma}\frac{\partial p}{\partial t} = -p\nabla(\alpha_2\mathbf{w}) + (\mathbf{w}, \mathbf{f}_1) + q_1. \tag{22}$$

Equations (21) and (22) define $\mathbf{w}$ and p. This is a system of quasi-linear equations of the first order of the hyperbolic type. The eigenvalues of the Jacobi matrix, which determine the propagation velocities of small disturbances, have the form

$$\lambda_{1,2} = \pm\lambda, \quad \lambda = \sqrt{\Gamma p\alpha_2\overline{\rho}/(\alpha_1\overline{\rho}_1\rho_2)}. \tag{23}$$

We write the system of equations (21), (22) in vector form

$$\begin{gathered}\frac{\partial\mathbf{Q}}{\partial t} + C\frac{\partial\mathbf{\Phi}}{\partial x} = \mathbf{S},\\ \mathbf{Q} = \begin{pmatrix} Q_1\\ Q_2\end{pmatrix} = \begin{pmatrix} \dfrac{\overline{\rho}_1\overline{\rho}_2}{\overline{\rho}}\mathbf{w}\\ \dfrac{\alpha_1}{\gamma-1}\ln p\end{pmatrix}, \quad \mathbf{\Phi} = \begin{pmatrix}\Phi_1\\ \Phi_2\end{pmatrix} = \begin{pmatrix} p\\ \alpha_2\mathbf{w}\end{pmatrix}, \quad \mathbf{S} = \begin{pmatrix}\mathbf{f}_2\\ \dfrac{\mathbf{w}\mathbf{f}_1 + q_1}{p}\end{pmatrix}, \quad C = \begin{pmatrix}\alpha_2 & 0\\ 0 & 1\end{pmatrix}.\end{gathered} \tag{24}$$

Due to the constancy of α_2 in a cell when writing a difference scheme

$$\mathbf{Q}_i^{n+1} = \mathbf{Q}_i^n - \frac{\Delta t C_i}{h}(\mathbf{\Phi}_{i+1/2} - \mathbf{\Phi}_{i-1/2}). \tag{25}$$

To approximate the numerical flow, we consider the Riemann problem:

$$\begin{gathered}\frac{\partial\mathbf{Q}}{\partial t} + C\frac{\partial\mathbf{\Phi}}{\partial x} = 0, \quad -\infty < x < +\infty,\\ \begin{cases}\mathbf{Q} = \mathbf{Q}_L, & \alpha_2 = \alpha_{2,L}, \quad x < 0,\\ \mathbf{Q} = \mathbf{Q}_R, & \alpha_2 = \alpha_{2,R}, \quad x \ge 0.\end{cases}\end{gathered} \tag{26}$$

We construct an approximate solution of the HLL-type problem. To do this, we define the velocities of the boundary waves of the disturbed region as

$$s_L = -\lambda(\alpha_{2,L}, \mathbf{Q}_L), \quad s_R = \lambda(\alpha_{2,R}, \mathbf{Q}_R). \tag{27}$$

We will look for a solution in the disturbed region in the form of a piecewise constant function

$$\mathbf{Q} = \begin{cases} \mathbf{Q}_L^*, & s_L \le x/t \le 0, \\ \mathbf{Q}_R^*, & 0 \le x/t \le s_R, \end{cases} \quad \mathbf{\Phi} = \mathbf{\Phi}^*, \quad s_L \le x/t \le s_R. \tag{28}$$

The structure of vectors $\mathbf{Q}_{L/R}^*$ is determined by the relations

$$\mathbf{Q}_{L/R}^* = \mathbf{B}_{L/R}\mathbf{Q}^*, \quad \mathbf{B}_{L/R} = \begin{pmatrix} \overline{\rho}_1\rho_2/\overline{\rho} & 0 \\ 0 & \alpha_1/(\gamma-1) \end{pmatrix}. \tag{29}$$

From the Rankine–Hugoniot relations on the waves bounding the disturbed region, we have

$$\begin{cases} s_L(\mathbf{Q}_L - B_L\mathbf{Q}^*) = C_L(\mathbf{\Phi}_L - \mathbf{\Phi}^*), \\ s_R(\mathbf{Q}_R - B_R\mathbf{Q}^*) = C_R(\mathbf{\Phi}_R - \mathbf{\Phi}^*). \end{cases} \tag{30}$$

Values $\mathbf{Q}^*$ and $\mathbf{\Phi}^*$ are defined as

$$\mathbf{Q}^* = \frac{\mathbf{C}_L\mathbf{F}_R - \mathbf{C}_R\mathbf{F}_L}{\mathbf{C}_R s_L\mathbf{B}_L - \mathbf{C}_L s_R\mathbf{B}_R}, \quad \mathbf{\Phi}^* = \frac{\mathbf{B}_L s_L\mathbf{F}_R - \mathbf{B}_R s_R\mathbf{F}_L}{\mathbf{C}_R s_L\mathbf{B}_L - \mathbf{C}_L s_R\mathbf{B}_R}, \tag{31}$$

where $\mathbf{F}_{L/R} = \mathbf{C}_{L/R}\mathbf{\Phi}_{L/R} - s_{L/R}\mathbf{Q}_{L/R}$. In the absence of k-phase in $\mathbf{Q}_{L/R}$, the flow value has a limit value of $\mathbf{\Phi}^* = \mathbf{\Phi}_{R/L}$. Comparing eigenvalues (9) and (23), we can find that the restriction on the time step at the stage under consideration is weaker than at the first stage in the case $\rho_1/\rho_2 < (1 + \alpha_2)/\alpha_2$, which is true for gases and solid particles under nonextreme conditions.

4. CALCULATION RESULTS

The proposed method is verified on a series of one-dimensional problems. We consider an ideal gas with the adiabatic exponent $\gamma = 1.4$. For particles, an approximation of intergranular pressure with parameters $\beta_* = 0.58$, $k = 0.57$, and $B = 0.15$ ([B] = MPa) [13] is used. The interfacial interaction $\mathbf{f}_k, q_k$ is neglected in the calculations because the properties of the basic numerical method are being studied.

In the first test, the ability of the numerical method to maintain the motion of a mixture of particles and gas at a constant velocity (the property of well-balancing) is verified. The second test demonstrates the formation of a compaction wave and a shock wave after reflection from a wall. The third test shows the formation of a rarefaction wave in the presence of particles. The fourth test considers the formation of a regular wave configuration in a region with a piecewise constant distribution of the volume fraction of particles. Numerical solutions are obtained for several values of the volume fraction of particles and are compared with the exact analytical solution for the case of the stationary phase of particles. In the fifth test, the interaction of a shock wave with a near-wall layer of light particles is numerically studied without taking into account the viscous interaction.

4.1. Convective Transport of a Flat Layer of Particles in a Gas

The movement of a backfill of particles with a subcritical volume fraction in a gas is considered. The gas and particles move at the same constant velocity towards an area without particles. The gas pressure in the region is constant, and the density undergoes a discontinuity at the boundary of the particle layer. The initial data of the problem are given in Table 1. The initial position of the layer boundary corresponds to $x = 0.05$ m. A uniform grid of 400 cells is used in the calculation. On the left boundary, the density, velocity, and pressure of the gas, as well as the volume fraction and velocity of the particles, are specified. On the right boundary, the interpolation condition is specified.

The calculation results are shown in Fig. 1. Here, the numerical solutions at the time $t = 0.1325$ ms are given. The area of the particle layer at this moment is [0.17, 0.87]. Due to numerical diffusion, the boundary of the particle region is smeared on the volume fraction distribution. The smeared width is greater than for calculations without gas. In this case, the particle velocity remains constant. The zero velocity values on the graph correspond to points with the zero-volume fraction.

Table 1. Initial parameters in the problem of transfer of a layer of particles with a gas

	$0 < x < 0.05$	$0.05 < x < 0.1$
α_2	0.5	0
u_2, km/s	0.2	0
ρ_1, kg/m^3	3.6	2.6
u_1, km/s	0.2	0.2
P_1, MPa	0.3	0.3

Table 2. Initial parameters in the problem of the formation of a compaction wave and a shock wave in a gas

	$0 < x < 0.1$
α_2	0.5
u_2, km/s	−0.2
ρ_1, kg/m^3	0.036
u_1, km/s	−0.2
P_1, MPa	0.3

4.2. Formation of a Particle Compaction Wave and a Shock Wave in a Gas

The flow of a mixture of gas and particles with the same velocity in the direction of an impermeable wall is considered. the flow rate of the particles and gas is given on the right boundary. The particles have a subcritical volume fraction and density of 100 kg/m^3. Table 2 shows the initial parameters of the problem. The computational domain is 0.1 m long and contains 800 cells.

Figure 2 shows the distribution of parameters after the shock wave is reflected from the wall. In the compaction wave, the volume fraction of particles rises to supercritical values of about 0.64, and the velocity decreases to zero. To the left of the compaction wave, a shock wave propagates in the gas.

4.3. Formation of a Rarefaction Wave in a Gas with Particles

The formation of a rarefaction wave in a mixture of particles with a gas is considered. The particles have a subcritical volume fraction and density of 100 kg/m^3. Table 3 shows the initial parameters of the prob-

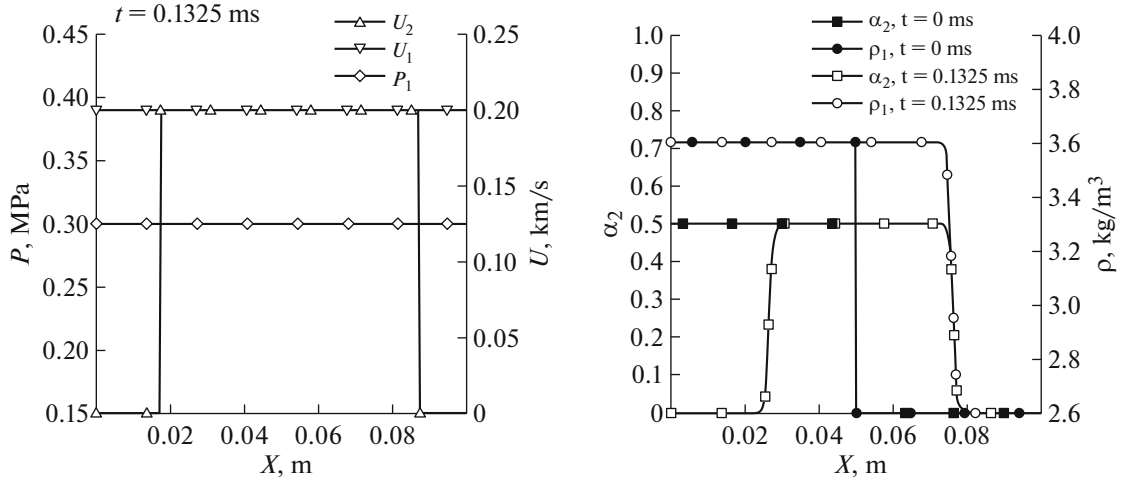

Fig. 1. Distribution of parameters in the computational domain at the moment of time $t = 0.1325$ ms.

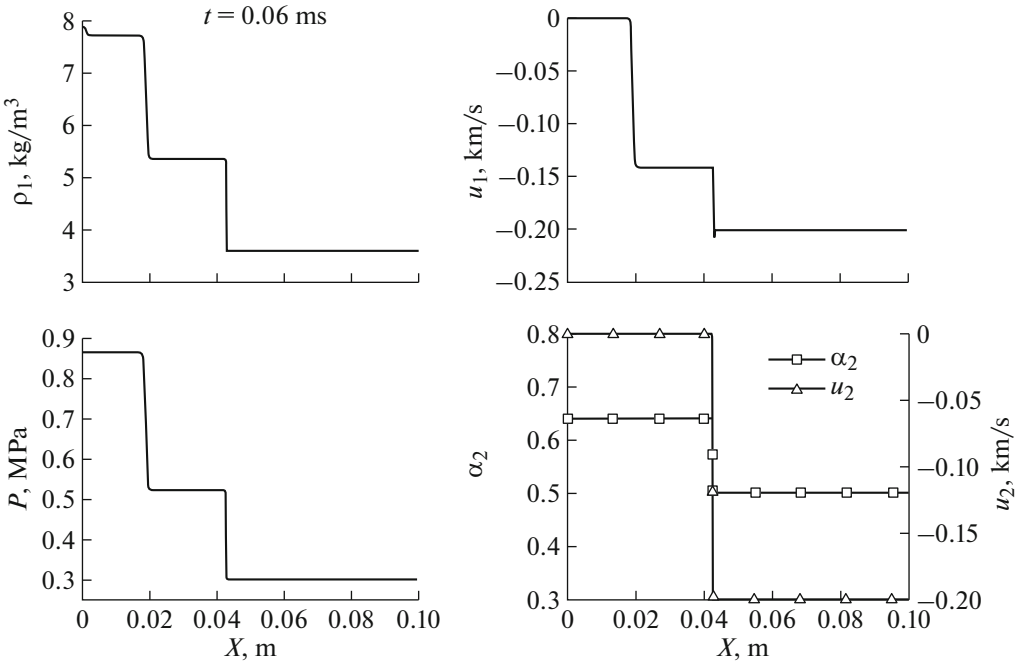

Fig. 2. Distribution of parameters in the problem of formation of a shock wave and a compaction wave.

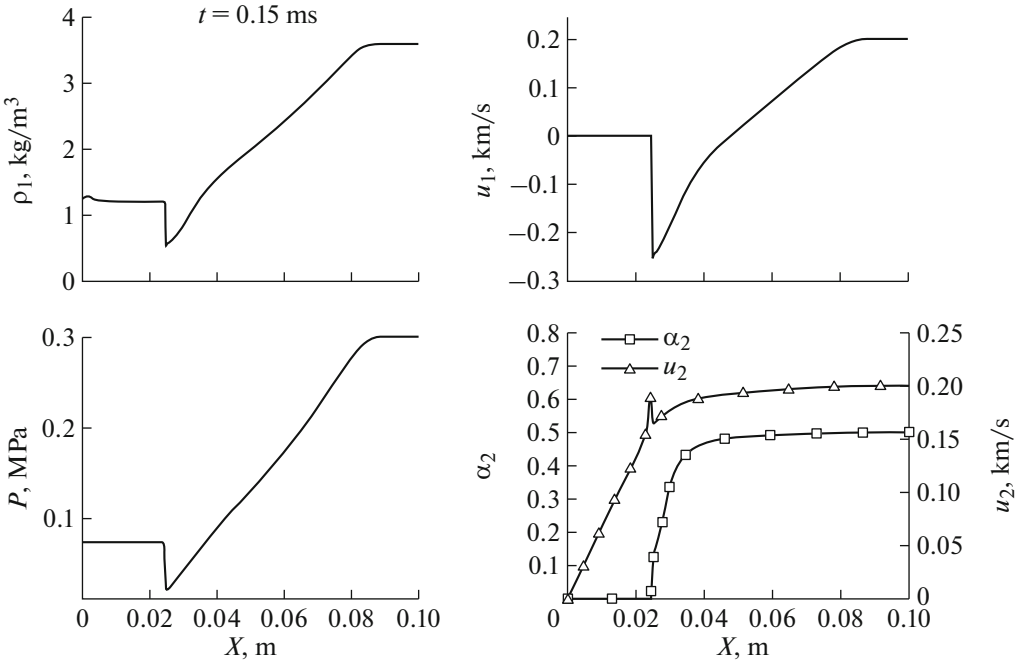

Fig. 3. Test with the formation of a rarefaction wave and an area without particles.

lem. The wall condition is specified on the left boundary of the region, and zero-order interpolation is specified on the right boundary. The computational domain is 0.1 m long and contains 800 cells.

Due to the subcritical initial volume fraction of the particles, a decompaction wave is not formed in the particle phase. The presence of a pressure gradient in a region with a nonzero volume fraction of particles (Fig. 3) leads to a distortion of the profile of gas parameters compared to a conventional rarefaction wave in a gas, as well as to a slowdown of particles in the near-wall region.

Table 3. Initial parameters in the problem of the formation of a rarefaction wave

	$0 < x < 0.05$
α_2	0.5
u_2, km/s	0.2
ρ_1, kg/m^3	0.036
u_1, km/s	0.2
P_1, MPa	0.3

Table 4. Initial parameters in the problem of the transfer of a layer of particles

	$0 < x < 0.8$	$x > 0.8$
α_2	0.1	0
u_2, km/s	0.0	0
ρ_1, kg/m^3	3.6	3.23885
u_1, km/s	0.1	0.153785
P_1, MPa	0.3	0.2

4.4. Decay of the Initial Discontinuity in a Mixture of Gas and Particles

This test is given for comparison with the reference solution, since there are no exact solutions in the literature for the considered system of equations (1). In [14], gas flows in regions with the given and time-constant distribution of the volume fraction are considered. These flows are actually described by two-phase equations in which the particle phase is stationary. Test C was chosen as the reference solution. The initial data for it are given in Table 4 and the exact solution is shown in Fig. 4 by the lines without symbols. The wave configuration resulting from the decay of the discontinuity in this test is regular; i.e., the resulting shock wave and rarefaction wave do not intersect with the porosity discontinuity. In model (1), the pressure drop leads to the appearance of the k-phase velocity. In order to compare the solution obtained by model (1) with the reference solution, solid-state particle densities of 10^2, 10^3, and 10^5 kg/m^3 are considered, since denser particles accelerate to a lower velocity. At a high density of the particles, they actually remain in place; thus, the resulting numerical solution must coincide with the exact reference solution. The calculations considered an area 2 m long containing 800 cells.

Figure 4 shows the results of the numerical calculations by the proposed method as lines with markers. The solutions obtained for different particle densities are close to each other. As the particle density increases, the value of the gas velocity between the rarefaction wave and the porosity discontinuity increases and approaches the value of the reference solution. In this case, the particle velocities decrease correspondingly. At a particle density of $\rho_2 = 10^5$ kg/m^3, the particle velocities in the calculation are $\sim 10^{-6}$ km/s.

4.5. Interaction of a Shock Wave with a Near-Wall Layer of Particles

In this test, we consider the impact of a shock wave with M = 2.73 on a layer of particles at rest located near the wall. The initial data for this problem are given in Table 5. The initial volume fraction and thick-

Table 5. Initial parameters in the problem of the interaction of a shock wave with a near-wall layer of particles

	$0 < x < 1.3$	$1.3 < x < 1.5$	$1.5 < x < 2.0$
α_2	0.0	0.0	0.5
u_2, km/s	0.0	0.0	0.0
ρ_1, kg/m^3	0.03405535	0.009483804	0.009483804
u_1, km/s	0.75184007	0.0	0.0
P_1, MPa	0.008528383	0.001	0.001

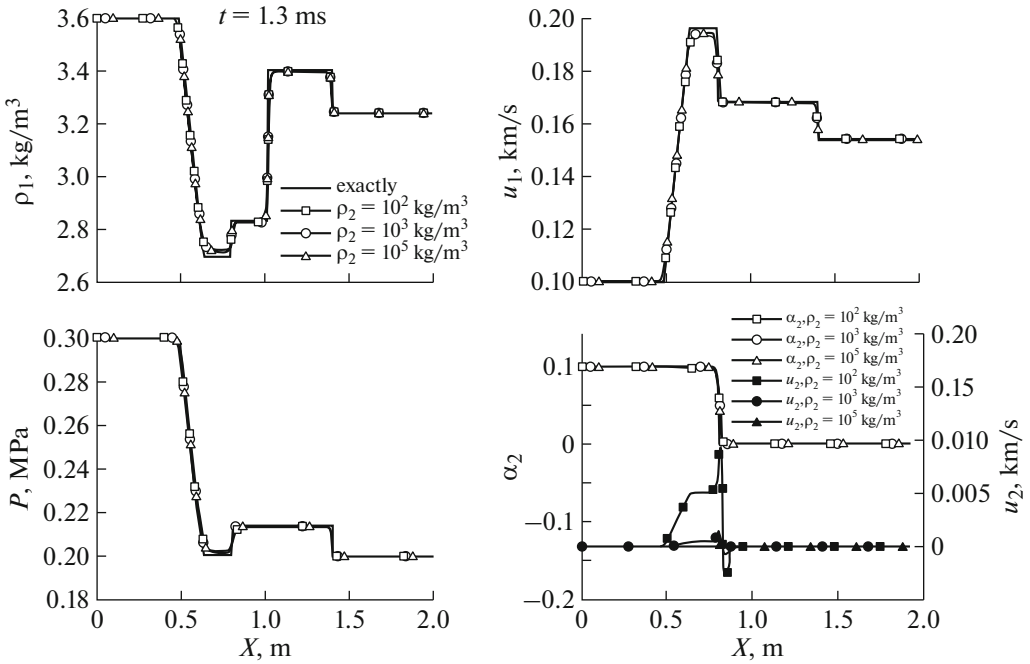

Fig. 4. Parameters in test C when varying particle density. The HLL method; scheme of increased order of accuracy. Comparison with the exact solution for stationary particles.

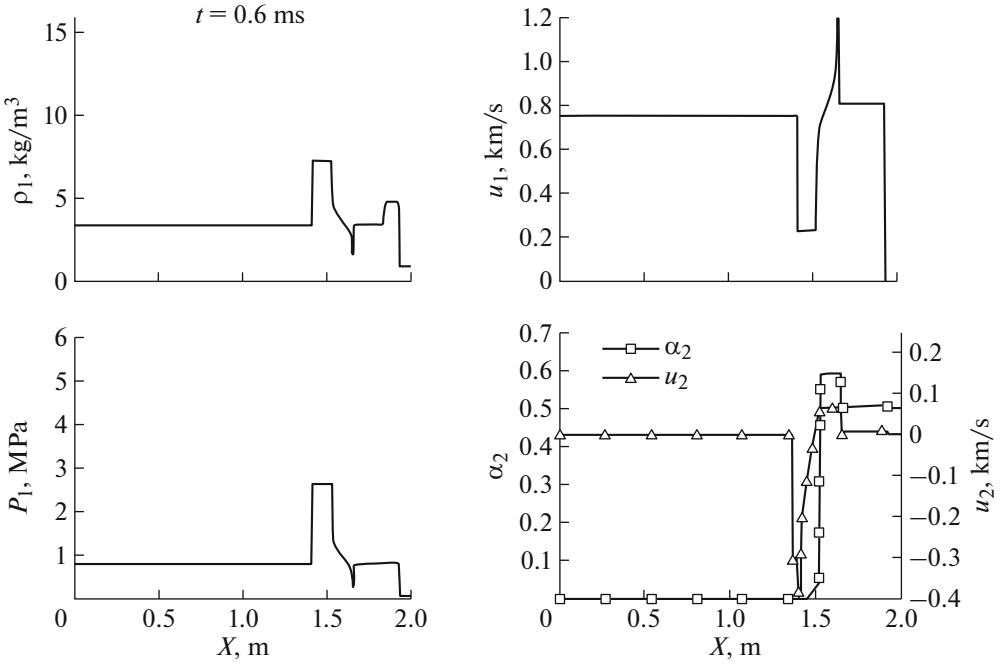

Fig. 5. Parameters in a test with a shock wave falling on a layer of particles after the formation of a compaction wave at the layer boundary. The HLL method; scheme of increased order of accuracy.

ness of the particle layer are 0.5 and 0.5 m, respectively. The computational domain has a length of 2 m and contains 1600 cells.

Figure 5 shows the distribution of parameters at time 0.6 ms. At this point, a reflected shock wave has formed in the gas, propagating to the left. Under the action of the pressure gradient in this wave, particles with a low volume fraction accelerate and also move to the left. In the backfill of particles, interfacial inter-

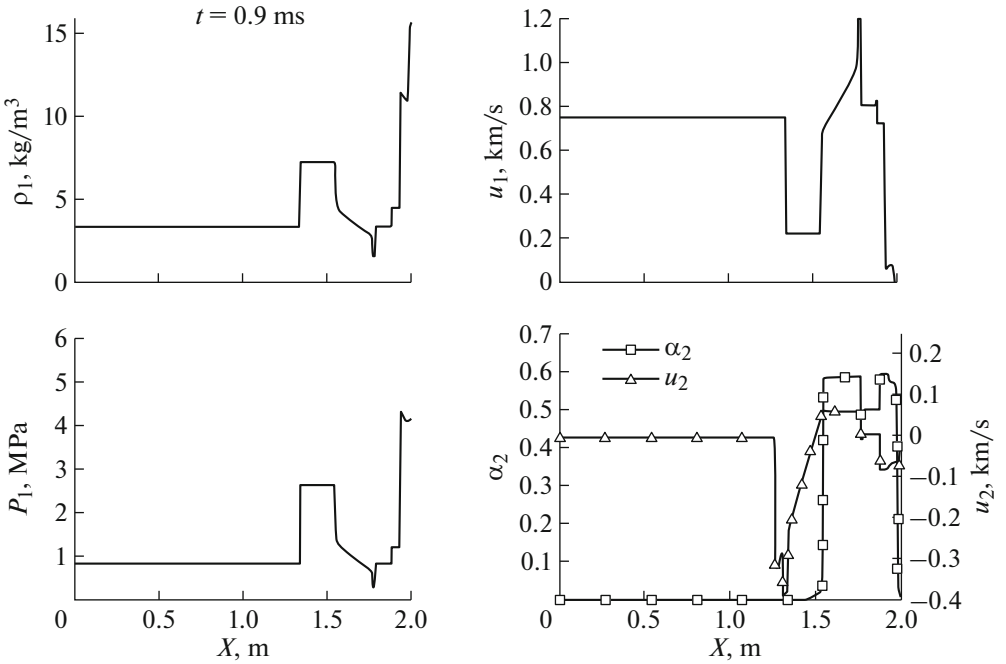

Fig. 6. Parameters in the test with shock wave incident on a layer of particles after reflection of the transmitted shock wave from the wall. The HLL method; scheme of increased order of accuracy.

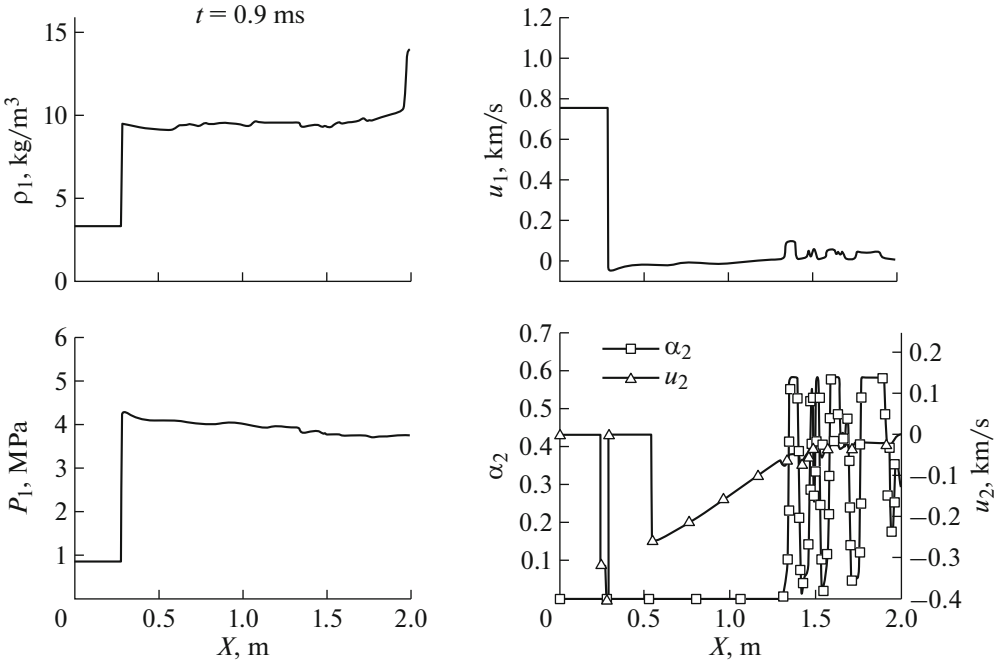

Fig. 7. Parameters in a test with a shock wave falling onto a layer of particles after the interaction of transmitted and reflected shock waves. The HLL method; scheme of increased order of accuracy.

action leads to the compaction of particles to a subcritical volume fraction and the appearance of a low positive velocity near the front of a passing shock wave. At the boundary of the layer of particles, by this moment, the transmitted shock wave has formed a compaction wave, in which the volume fraction of particles increases to a supercritical volume. The propagation of a compaction wave in the presence of interfacial interaction leads to the formation of a gas velocity peak.

Figure 6 shows the distribution of parameters at time 0.9 ms. At this point, the passing shock wave was reflected from the wall. Under the influence of this wave, particles were compacted to a volume fraction above critical. In this case, the particles near the wall move with negative velocity. On the right boundary of this layer, a decompaction wave has already formed, in which the volume fraction decreases to the critical one. On the decompaction wave, the gas parameters undergo a discontinuity.

Figure 7 shows the distribution of parameters at 4.0 ms. Near the reflected shock wave, a cloud of particles with a low volume fraction, separate from the main backfill, was formed. The interaction of compaction waves led to the delamination of particles (the effect of the fragmentation a cloud of particles) and the motion of the resulting layers in the direction from the wall.

CONCLUSIONS

This paper proposes a method for regularizing a mathematical model of the flow of a two-phase mixture of gas and solid particles. The model of R.I. Nigmatulin is considered as a mathematical model under the assumption of absolutely rigid, incompressible, and nondeformable particles. The regularization method is based on splitting the original system into two subsystems that describe, respectively, the dynamics of the phases and the interphase interaction. For each of the resulting systems, which are hyperbolic and have a conservative form, a Godunov-type method is constructed based on an approximate HLL solution to the Riemann problem. For the first system, a numerical method of a higher approximation order is constructed.

The proposed numerical method was verified on a series of problems that admit exact solutions. The results of the test calculations showed the ability of the numerical method to keep the movement of the mixture at a constant velocity, as well as close agreement with the exact analytical solutions in terms of the quantitative wave characteristics (amplitude, wave and characteristics propagation velocity).

The interaction of a shock wave with a near-wall layer of particles was simulated without taking into account relaxation values in velocity. The effect of the stratification of a homogeneous backfill of light particles under the influence of a passing shock wave and the resulting compaction and decompaction waves was obtained.

ACKNOWLEDGMENTS

The author thanks Dr. Igor Stanislavovich Menshov for his valuable recommendations and comments during the preparation of the article.

FUNDING

This study was carried out as part of a state assignment of the Scientific Research Institute of System Analysis, Russian Academy of Sciences on the topic FNEF-2022-0005 (registration no. 1021060708369-1-1.2.1) "Mathematical modeling of dynamic processes in deformable and reacting media using multiprocessor computing systems." This study was carried out with the financial support from the Russian Foundation for Basic Research as part of scientific project no. 20-31-90027 ("Graduate Students").

CONFLICT OF INTEREST

The author of this work declares that he has no conflicts of interest.

REFERENCES

1. H. Arastoopour, D. Gidaspow, and R. Lyczkowski, *Transport Phenomena in Multiphase Systems*, Mechanical Engineering Series (Springer, Cham, 2022). https://doi.org/10.1007/978-3-030-68578-2
2. D. Gao, G. Zhou, R. Liu, S. Li, Ya. Kong, and Yo. Wang, "CFD investigation on gas–solid two-phase flow of dust removal characteristics for cartridge filter: A case study," Environ. Sci. Pollut. Res. **28**, 13243–13263 (2021). https://doi.org/10.1007/s11356-020-11334-6
3. Yu. P. Khomenko, A. N. Ishchenko, and V. Z. Kasimov, *Mathematical Modeling of Intraballistic Processes in Barelled Systems*, Ed. by Yu. P. Khomenko (Izd-vo Sib. Otd. Ross. Akad. Nauk, Novosibirsk, 1999).

4. C. K. Man and M. L. Harris, "Participation of large particles in coal dust explosions," J. Loss Prevention Process Industries **27**, 49–54 (2014). https://doi.org/10.1016/j.jlp.2013.11.004
5. F. E. Marble, "Dynamics of a gas containing small solid particles," in *Combustion and Propulsion: 5th AGARDograph Colloquim* (Pergamon Press, Oxford, 1963).
6. A. N. Kraiko and L. E. Sternin, "Theory of flows of a two-velocity continuous medium containing solid or liquid particles," J. Appl. Math. Mech. **29**, 482–496 (1965). https://doi.org/10.1016/0021-8928(65)90059-6
7. R. I. Nigmatulin, *Dynamics of Multiphase Media* (Nauka, Moscow, 1987).
8. D. Gidaspow, *Multiphase Flow and Fluidization: Continuum and Kinetic Theory Descriptions* (Academic, 1994).
9. M. Baer and J. Nunziato, "A two-phase mixture theory for the deflagration-to-detonation transition (ddt) in reactive granular materials," Int. J. Multiphase Flow **12**, 861–889 (1986). https://doi.org/10.1016/0301-9322(86)90033-9
10. Poroshina Ya and P. Utkin, "Numerical simulation of interaction of the normally incident shock wave with a layer of particles using Baer–Nunziato system of equations," Gorenie Vzryv **13**, 95–104 (2020).
11. A. V. Rodionov, "Monotonic scheme of the second order of approximation for the continuous calculation of non-equilibrium flows," USSR Comput. Math. Math. Phys. **27**, 175–180 (1987). https://doi.org/10.1016/0041-5553(87)90174-1
12. B. Einfeldt, C. Munz, P. Roe, and B. Sjögreen, "On Godunov-type methods near low densities," J. Comput. Phys. **92**, 273–295 (1991). https://doi.org/10.1016/0021-9991(91)90211-3
13. M. Y. Nemtsev, I. S. Menshov, and I. V. Semenov, "Numerical simulation of dynamic processes in a medium of fine-grained solid particles," Math. Models Comput. Simul. **15**, 210–226 (2023). https://doi.org/10.1134/s2070048223020138
14. S. Clain and D. Rochette, "First- and second-order finite volume methods for the one-dimensional nonconservative Euler system," J. Comput. Phys. **228**, 8214–8248 (2009). https://doi.org/10.1016/j.jcp.2009.07.038